2008 IEEE International Conference on
Robotics and Automation
Pasadena, CA, USA, May 19-23, 2008

Navigation of an Omni-directional Mobile Robot with Active Caster Wheels

Eui-jung Jung, Ho Yul Lee, Jae Hoon LEE, Byung-Ju Yi, *Member, IEEE,*
Whee Kuk Kim, *Member, IEEE,* and Shin'ichi Yuta, *Member, IEEE*

Abstract—**This work deals with navigation of an omni-directional mobile robot with active caster wheels. Initially, the posture of the omni-directional mobile robot is calculated by using the odometry information. Next, the position accuracy of the mobile robot is measured through comparison of the odometry information and the external sensor measurement. Finally, for successful navigation of the mobile robot, a motion planning algorithm that employs kinematic redundancy resolution method is proposed. Through experiments for multiple obstacles and multiple moving obstacles, the feasibility of the proposed navigation algorithm was verified.**

I. Introduction

The types of wheels used in most of mobile robots can be classified as four different types; conventional wheel, centered orientable wheel, off-centered caster wheel, and Swedish wheel[1-3]. For the mobile robot to have an omni-directional characteristic on the plane, only wheels with three degrees of freedom must be employed in mobile robots. Either the caster wheel or Swedish wheel can be modeled kinematically as three degree of freedom serial chain. Chen, et al.[4] developed an omni-directional mobile robot using the crawler with free roller. Tadakuma, et al.[5] implemented an omni-directional mobile robot including omni-disk using the passive wheel. Ziaie-Rad, et al. [6] developed Perisia omni-directional soccer player robot with 6 omni-wheels. Salih, et al.[7] developed an omni-directional mobile robot using four custom-made mecanum wheels.

However, it is known that either Swedish wheel or most of other type of "omni-directional wheels" are very sensitive to road conditions, and thus their operational performances are more or less limited, compared to conventional wheels.

On the other hand, the active caster wheel is not sensitive to road conditions and also is able to overcome a sort of steps encountered in uneven floors by using the active driving wheel. Recently, researches on omni-directional mobile robots with active caster wheels have drawn much attention. Moore and Flann[8] and Berkermeier and Ma[9] implemented a six-wheeled omni-directional mobile robot and ODIS (Omni-Directional Inspection System) with the so-called "smart wheel" active caster wheel module, respectively. Yi and Kim [13] initially developed the kinematic model of the omni-directional mobile robot with active caster wheels. Wada, et al.[10] developed the mobile robot with two caster wheels and one rotational actuator. Ushimi, et al.[11] developed an omni-directional vehicle with two-wheeled casters. Lee, et al.[12] implemented and proposed a motion generation algorithm for the caster-type omni-directional mobile robot. Park, et al. [16] addressed the optimal design for this type of mobile robots.

There are many researches on mobile robot navigation. However, navigation of the omni-directional mobile robots was rarely studied. Zavlangas, et al.[17] implemented this issue to a Swedish wheel type mobile robot, but it is not completely reliable because of accumulated odometry errors. If odometry information is not reliable, the mobile should depend on external sensor for navigation.

In light of these facts, this paper initially reviews a kinematic model of the mobile robots with three active caster wheels. Then, we propose an algorithm to obtain reliable odometry information geometrically by multiple encoder information, and we also show the effectiveness of the proposed algorithm through experimentation. Finally, we implement navigation algorithm to an omni-directional mobile, which employs kinematic redundancy resolution algorithm to avoid obstacles and reach to the goal position.

II. Kinematic Modeling

A. Mobility Analysis

Mobility is known as the number of minimum input parameters required to specify all the locations of the system relative to another. Grübler's formula describing mobility is given [15] by

$$M = N(L-1) - \sum_{i=1}^{J}(N - F_i), \quad (1)$$

where N is the dimensions of the allowable motion space spanned by all joints, L is the link number, J is the joint number and F_i is the motion degree of freedom of the i-th joint. Consider a three-wheeled mobile robot shown in Fig.

E.-J. Jung is with School of Electrical Engineering and Computer Science, Hanyang University, Korea. (e-mail : jeuij79@naver.com)
H. Y. Lee is with School of Electrical Engineering and Computer Science, Hanyang University, Korea. (e-mail : 80c196@korea.com)
J. H. LEE is with Ubiquitous Functions Research Group, Intelligent Systems Research Institute, AIST, Japan. (e-mail : jh.lee@aist.go.jp)
B.-J. Yi is with School of Electrical Engineering and Computer Science, Hanyang University, Korea. (e-mail : bj@hanyang.ac.kr)
W.K. Kim is with Department of Control and Instrumentation Engineering, Korea University, Korea (e-mail : wheekuk@korea.ac.kr)
S. Y is with Institute of Engineering Mechanics and Systems, University of Tsukuba, Japan (yuta@roboken.esys.tsukuba.ac.jp)

978-1-4244-1647-9/08/$25.00 ©2008 IEEE.

1(a).

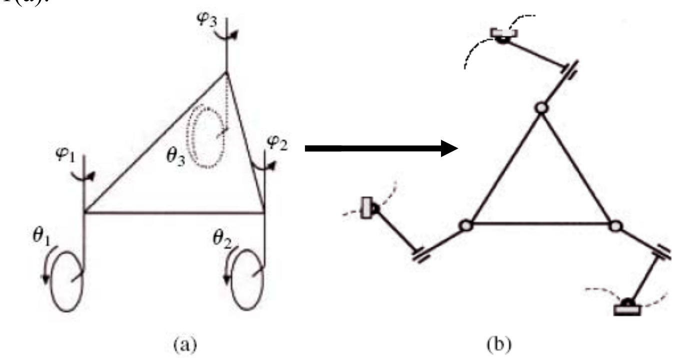

Fig. 1. Modeling of Omni-directional mobile robot

We assume that every wheel retains point contact at the ground, and that the wheel does not slip in the horizontal direction, but it is allowed to rotate about the vertical axis. Each wheel mechanism possesses its own driving and steering actuators. Then, the instantaneous motion of each wheel mechanism can be modeled as two revolute joints and one prismatic joint, as shown in Fig.1(b). Mobility of the omni-directional mobile robot can be calculated as below.

$$M = 3(8-1) - \sum_{i=1}^{9}(3-1) = 3 \tag{2}$$

B. First-order Kinematics

Consider the mobile robot depicted in Fig. 2. This system consists of three wheels, three offset link, and a top platform. Assume that the motion of the mobile robot is constrained to the plane and there exists no sliding and skidding friction, but that rotation of the wheel about the axis vertical to the ground is allowed. XYZ represents the global reference frame, and xyz denotes a local coordinate frame attached to the mobile platform; **i, j,** and **k** are the unit vectors of the xyz coordinate frame. C denotes the origin of the local coordinate.

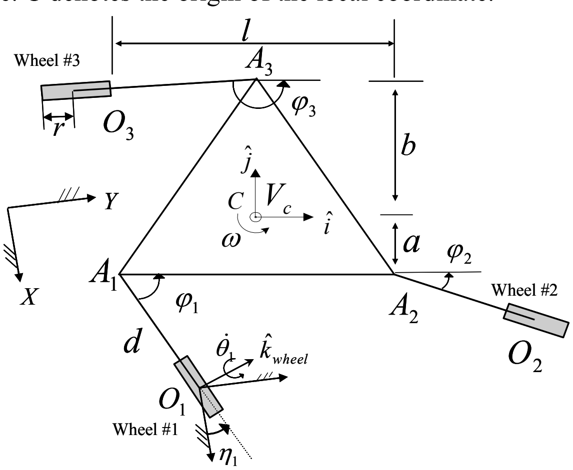

Fig. 2. Kinematics description of the omni-directional mobile robot

We define θ as the rotating angle of the wheel and φ as the steering angle between the steering link and the local x-axis. η denotes the angular displacement of the wheel relative to the X-axis of the global reference frame. r and d denote the radius of the wheel and the length of the steering link, respectively.

The linear velocities at the center of the wheels are given as

$$\mathbf{v}_{oi} = \dot{\theta}_i\left(\sin\varphi_i\mathbf{i} + \cos\varphi_i\mathbf{j}\right)\times r\mathbf{k} \quad i = \mathbf{1,2,3}\,. \tag{3}$$

The linear velocity at C of the mobile robot can be described as

$$\begin{aligned}\mathbf{v}_c &= \mathbf{v}_{o1} + \dot{\eta}_1\mathbf{k}\times\overrightarrow{O_1A_1} + \omega\mathbf{k}\times\overrightarrow{A_1C}\\ &= \dot{\theta}_1\left(\sin\varphi_1\mathbf{i} + \cos\varphi_1\mathbf{j}\right)\times r\mathbf{k}\\ &\quad + \dot{\eta}_1\mathbf{k}\times\left(-d\cos\varphi_1\mathbf{i} + d\sin\varphi_1\mathbf{j}\right),\\ &\quad + \omega\mathbf{k}\times\left(\frac{l}{2}\mathbf{i} + a\mathbf{j}\right)\end{aligned} \tag{4}$$

$$\begin{aligned}\mathbf{v}_c &= \mathbf{v}_{o2} + \dot{\eta}_2\mathbf{k}\times\overrightarrow{O_2A_2} + \omega\mathbf{k}\times\overrightarrow{A_2C}\\ &= \dot{\theta}_2\left(\sin\varphi_2\mathbf{i} + \cos\varphi_2\mathbf{j}\right)\times r\mathbf{k}\\ &\quad + \dot{\eta}_2\mathbf{k}\times\left(-d\cos\varphi_2\mathbf{i} + d\sin\varphi_2\mathbf{j}\right),\\ &\quad + \omega\mathbf{k}\times\left(-\frac{l}{2}\mathbf{i} + a\mathbf{j}\right)\end{aligned} \tag{5}$$

and

$$\begin{aligned}\mathbf{v}_c &= \mathbf{v}_{o3} + \dot{\eta}_3\mathbf{k}\times\overrightarrow{O_3A_3} + \omega\mathbf{k}\times\overrightarrow{A_3C}\\ &= \dot{\theta}_3\left(\sin\varphi_3\mathbf{i} + \cos\varphi_3\mathbf{j}\right)\times r\mathbf{k}\\ &\quad + \dot{\eta}_3\mathbf{k}\times\left(-d\cos\varphi_3\mathbf{i} + d\sin\varphi_3\mathbf{j}\right),\\ &\quad + \omega\mathbf{k}\times\left(\text{-b}\mathbf{j}\right)\end{aligned} \tag{6}$$

where ω representing the angular velocity of the mobile platform can be described as

$$\omega = \dot{\eta}_i + \dot{\varphi}_i \quad i = 1,2,3\,. \tag{7}$$

$\mathbf{v}_c = \begin{bmatrix} v_{cx} & v_{cy} \end{bmatrix}^T$ of (4)-(6) and ω of (7) can be expressed as one matrix form given by

$$\dot{\mathbf{u}} = \begin{bmatrix} -d\sin\varphi_1 - a & r\cos\varphi_1 & -a \\ -d\cos\varphi_1 + l/2 & -r\sin\varphi_1 & l/2 \\ 1 & 0 & 1 \end{bmatrix}\begin{bmatrix}\dot{\eta}_1\\ \dot{\theta}_1\\ \dot{\varphi}_1\end{bmatrix}, \tag{8}$$

$$\dot{\mathbf{u}} = \begin{bmatrix} -d\sin\varphi_2 - a & r\cos\varphi_2 & -a \\ -d\cos\varphi_2 - l/2 & -r\sin\varphi_2 & -l/2 \\ 1 & 0 & 1 \end{bmatrix}\begin{bmatrix}\dot{\eta}_2\\ \dot{\theta}_2\\ \dot{\varphi}_2\end{bmatrix}, \tag{9}$$

and

$$\dot{\mathbf{u}} = \begin{bmatrix} -d\sin\varphi_3 + b & r\cos\varphi_3 & b \\ -d\cos\varphi_3 & -r\sin\varphi_3 & 0 \\ 1 & 0 & 1 \end{bmatrix}\begin{bmatrix}\dot{\eta}_3\\ \dot{\theta}_3\\ \dot{\varphi}_3\end{bmatrix}, \tag{10}$$

where the operational velocity vector is defined as

$$\dot{\mathbf{u}} = \begin{bmatrix} v_{cx} \\ v_{cy} \\ \omega \end{bmatrix}. \tag{11}$$

From (8) through (10), the mobile robot can be visualized as a parallel mechanism. The variable (η) interfacing the wheel to the ground enables this model. Thus, the kinematics of the mobile robot is instantaneously equivalent to that of typical parallel robot that is connected to a fixed ground.

The intermediate coordinate transfer method [14], which was popularly employed in parallel robot community, will be employed to derive the forward kinematic relation. Taking the inverses of (8)-(10), we have

$$\begin{bmatrix} \dot{\eta}_1 \\ \dot{\theta}_1 \\ \dot{\varphi}_1 \end{bmatrix} = \frac{1}{dr} \begin{bmatrix} -r\sin\varphi_1 & -r\cos\varphi_1 & \frac{l}{2} r\cos\varphi_1 - ar\sin\varphi_1 \\ d\cos\varphi_1 & -d\sin\varphi_1 & \frac{l}{2} d\sin\varphi_1 + ad\cos\varphi_1 \\ r\sin\varphi_1 & r\cos\varphi_1 & dr + ar\sin\varphi_1 - \frac{l}{2} r\cos\varphi_1 \end{bmatrix} \dot{\mathbf{u}} \tag{12}$$

$$\begin{bmatrix} \dot{\eta}_2 \\ \dot{\theta}_2 \\ \dot{\varphi}_2 \end{bmatrix} = \frac{1}{dr} \begin{bmatrix} -r\sin\varphi_2 & -r\cos\varphi_2 & \frac{l}{2} r\cos\varphi_2 - ar\sin\varphi_2 \\ d\cos\varphi_2 & -d\sin\varphi_2 & -\frac{l}{2} d\sin\varphi_2 + ad\cos\varphi_2 \\ r\sin\varphi_2 & r\cos\varphi_2 & dr + ar\sin\varphi_2 + \frac{l}{2} r\cos\varphi_2 \end{bmatrix} \dot{\mathbf{u}} \tag{13}$$

and

$$\begin{bmatrix} \dot{\eta}_3 \\ \dot{\theta}_3 \\ \dot{\varphi}_3 \end{bmatrix} = \frac{1}{dr} \begin{bmatrix} -r\sin\varphi_3 & -r\cos\varphi_3 & br\sin\varphi_3 \\ d\cos\varphi_3 & -d\sin\varphi_3 & -bd\cos\varphi_3 \\ r\sin\varphi_3 & r\cos\varphi_3 & dr - br\sin\varphi_3 \end{bmatrix} \dot{\mathbf{u}} \,. \tag{14}$$

Since the omni-directional mobile robot has mobility 3, we can define three minimum (or independent) coordinates. However, only three inputs are not enough to avoid singularity. Campion, et al.[1] and Yi and Kim[12] addressed that at least, two active wheels (i.e., two driving and two steering motors) are necessary. In our system, we employ three active wheels (six actuators). Thus, the system has force redundancy. In the equations (11) through (13), $\theta_1, \theta_2, \theta_3$ and $\varphi_1, \varphi_2, \varphi_3$ are the active joint variables. For a given operational velocity vector $\dot{\mathbf{u}}$, the system tries to follow the calculated joint angular velocities in real time.

III. ANALYSIS OF ODOMETER

A. Geometric Analysis

For navigation, mobile robots should know where they are. One of fundamental methods for this issue is using its odometer that can be calculated geometrically.

Fig. 3 shows the omni-directional mobile robot that was designed as an experimental platform. Each serial chain has 3-DOF in the kinematic model, but it has only two encoders which measure φ_i and θ_i as shown in Fig. 4. In this mechanism, φ_i and θ_i are motor-driven joints, and η_i is a passive joint.

The posture of the mobile robot can be described in terms of the two coordinates x and y of the origin C of the moving frame and the orientation angle ϕ of the moving frame, both with respect to the global frame with origin at G. Hence, the posture of the mobile robot is given by the (3×1) vector.

$$\xi = \begin{bmatrix} x \\ y \\ \phi \end{bmatrix} . \tag{15}$$

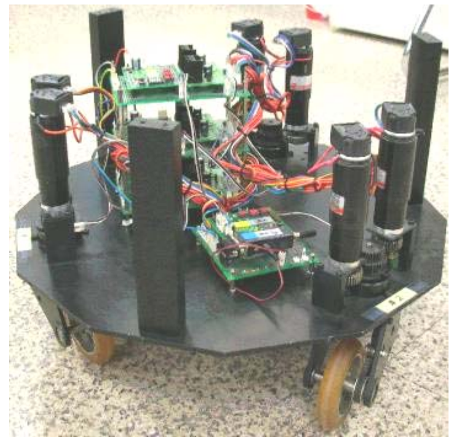

Fig. 3. The omni-directional mobile robot with active caster wheels

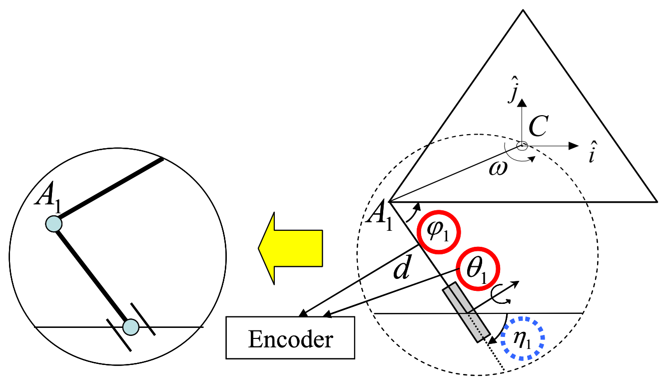

Fig. 4. Time-varying parameters determined by encoders

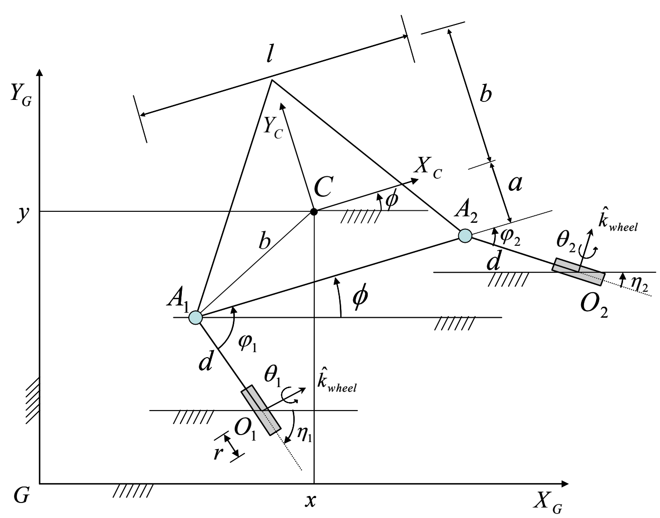

Fig. 5. Posture of the omni-directional mobile robot

The posture (i.e., position and orientation with respect to the global reference frame) of the mobile robot can be obtained by the encoder information (φ_i and θ_i) of the two chains as described in Fig.5. The rotation of the caster wheel with respect to the base frame, which is represented by the angle η_i, can be expressed as

$$\eta_i = \varphi_i - \phi . \quad (16)$$

Then if ϕ is given, then the robot posture can be determined as follows.

Step 1. Set the initial positions (O_1, O_2) of the wheels and angles of the caster wheels.

$$\begin{aligned} &O_1 : (x_{O1}, y_{O1}) \; O_2 : (x_{O2}, y_{O2}) \\ &\eta_i[0] = \varphi_i[0] = \theta_i[0] = 0 \\ &x_{O1}[0] = d - l/2, \quad y_{O1}[0] = -a \; . \\ &x_{O2}[0] = d + l/2, \quad y_{O2}[0] = -a \end{aligned} \quad (17)$$

Step 2. Update the positions of the caster wheels

$$\begin{aligned} x_{O1}[n+1] &= x_{O1}[n] + r\Delta\theta \cos(\eta_1[n]) \\ y_{O1}[n+1] &= y_{O1}[n] - r\Delta\theta \sin(\eta_1[n]) \\ x_{O2}[n+1] &= x_{O2}[n] + r\Delta\theta \cos(\eta_2[n]) \\ y_{O2}[n+1] &= y_{O2}[n] - r\Delta\theta \sin(\eta_2[n]) \end{aligned} \quad (18)$$

Step 3. Calculate the positions of the steering joints

$$\begin{aligned} &A_1 : (x_1, y_1) \quad A_2 : (x_2, y_2) \\ &x_1 = x_{O1} - d\cos(\eta_1), \quad y_1 = y_{O1} + d\sin(\eta_1) \\ &x_2 = x_{O2} - d\cos(\eta_2), \quad y_2 = y_{O2} + d\sin(\eta_2) \end{aligned} \quad (19)$$

Step 4. Obtain the posture of the mobile robot

$$\begin{aligned} &C : (x_c, y_c) \\ &x_c = x_1 + b\cos\left(\frac{\pi}{6} + \phi\right) \\ &y_c = y_1 + b\sin\left(\frac{\pi}{6} + \phi\right) \\ &\phi = atan2\left((y_2 - y_1), (x_2 - x_1)\right) \end{aligned} \quad (20)$$

The odometry information of the omni-directional mobile robot with active caster wheels can be obtained by using this procedure at every encoder sampling time iteratively.

B. Experiment

In order to evaluate the performance of the proposed method for odometer, an experiment is conducted for a rectangular trajectory. In experiment, we measure the real position of the mobile robot by using a laser range finder that is fixed at a certain position of the global frame. Fig. 6 displays the external measurement system, and the specification of the laser range finder is shown in Table I. The two coordinates x and y of the origin C of the moving frame are the center position of the vertical plate on the top of mobile robot. Fig. 7 shows the positions of the vertical plate in the laser range finder frame during the path following. Fig. 8 shows external measurement of the vertical plate, which is transformed to the global frame by (21). The horizontal bar denotes the shape of the vertical plate.

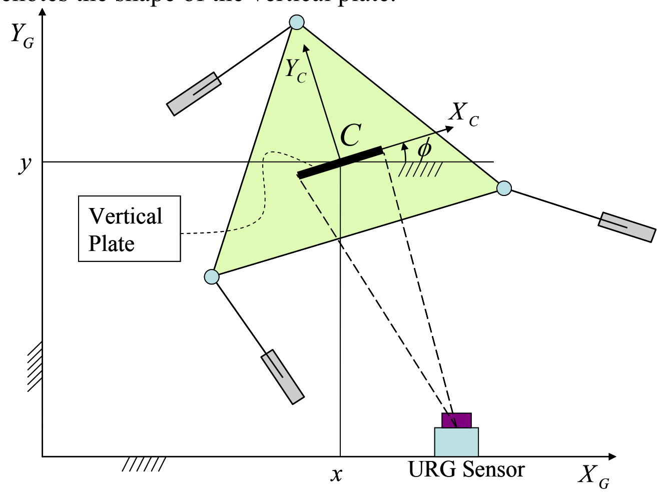

Fig. 6. External measurement system using a laser range finder

TABLE I
SPECIFICATION OF THE LASER RANGE FINDER

Model	URG-04LX(HOKUYO Co.)
Measurement Range	20~4000 mm
Measurement Resolution	1 mm
Angular Range	240 deg
Angular Resolution	0.3515625 deg

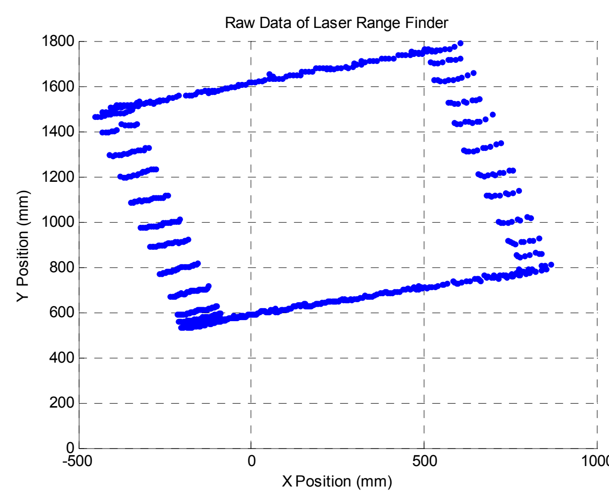

Fig. 7. Positions of the vertical plate in the laser range finder frame

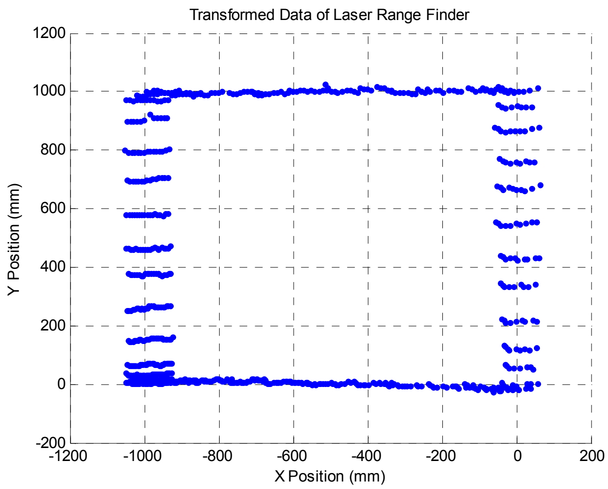

Fig. 8. Positions of the vertical plate in the global frame

$$\begin{bmatrix} x \\ y \end{bmatrix} = \begin{bmatrix} \cos(\theta) & -\sin(\theta) \\ \sin(\theta) & \cos(\theta) \end{bmatrix} \begin{bmatrix} x_L \\ y_L \end{bmatrix} + \begin{bmatrix} \Delta x \\ \Delta y \end{bmatrix}, \quad (21)$$

where θ denotes the rotation of the laser sensor frame with respect to the global frame, and x_L and y_L denote coordinates in the laser sensor frame, and Δx and Δy denote the position of the laser sensor in the global coordinate frame. Fig. 9 shows the trajectory following property of the omni-directional mobile robot. In the result of rectangular trajectory tracking control, the solid line denotes the given trajectory, the dotted line denotes the position history of the mobile robot measured by odometer inside the robot, and the dashed line denotes the position history measured by a URG laser sensor from outside. The external measurement depicted in Fig. 9 is the collection of the center points of the horizontal bars of Fig. 8. Although there are some noises owing to resolution of the LRF sensor, it is proved that the omni-directional mobile robot has a good tracking performance of the given rectangular trajectory. Fig. 10 shows the odometry error near the global origin position after the path following. $1cm$ error occurs after traveling $4m$. All forms of mobile robots cannot help having such odometry errors. The mobile robot we developed has more complicated structure compared with differential wheel type, which means that it can have more complicated systematic odometry error. Correction of systematic odometry errors in the omni-directional mobile robot is a future work.

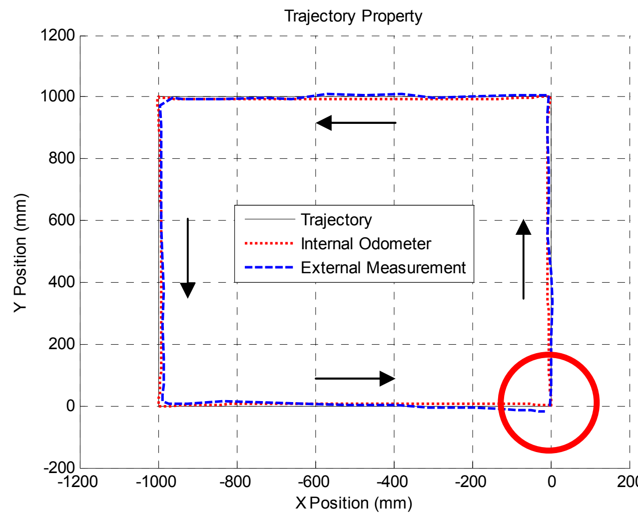

Fig. 9. Trajectory property of the omni-directional mobile robot.

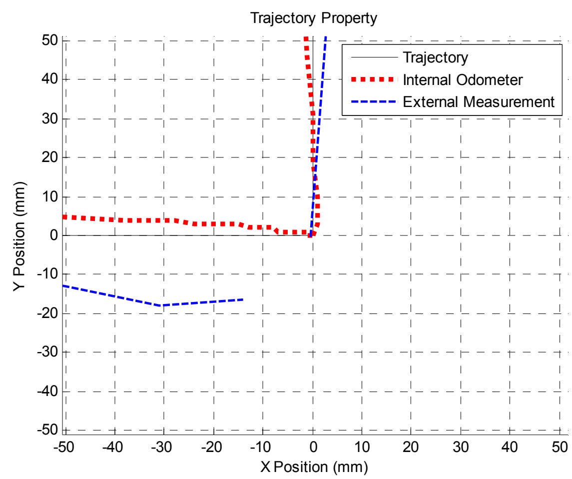

Fig. 10. Odometry error of the omni-directional mobile robot.

IV. Navigation

A. Navigation Algorithm

For navigation, mobile robots should know their postures with respect to the global reference frame as well as the positions of obstacles. Because the mobile robot we developed has 3-DOF, more dexterous motion to avoid obstacle is possible as compared to the differential type mobile robot. The first goal of navigation will be moving to the goal point, and then the second goal will be avoiding obstacles. To satisfy these purposes, positions of the mobile robot, obstacles, and goal point should be estimated. The navigation algorithm ought to minimize the distance between the current position of the mobile robot and the goal point, and maximizes the distances between the current position of the mobile robot and obstacles. The performance indices are set as follows.

$$\min\{P_G = (x - x_G)^2 + (y - y_G)^2\}$$
$$\max\{P_i = (x - x_i)^2 + (y - y_i)^2\}, \quad (22)$$

where x and y denote the positions of the mobile robot, x_G and y_G denote the positions of the goal point, and x_i and y_i denote the positions of the *i-th* obstacle.

Here, we would like to model the motion of the omni-directional mobile robot as a kinematically redundant robot. Initially, we set up the angular velocity of the mobile platform as the operational velocity as follows.

$$\dot{\mathbf{u}} = \omega = J \begin{bmatrix} v_{cx} \\ v_{cy} \\ \omega \end{bmatrix}, \quad (23)$$

where $J = \begin{bmatrix} 0 & 0 & 1 \end{bmatrix}$ and $\begin{bmatrix} v_{cx} & v_{cy} & \omega \end{bmatrix}^T$ denotes the velocity of the mobile platform with respect to the global reference frame. The general solution for (23) is given by

$$\begin{bmatrix} v_{cx} \\ v_{cy} \\ \omega \end{bmatrix} = J^{+}\dot{\mathbf{u}} + \left(\left[I\right] - J^{+}J\right)\nabla H, \quad (24)$$

where H defined in the homogeneous solution is the potential function that needs to be optimized. When the gradient of H is given as follows

$$\nabla H = \left(-K_G \frac{\partial P_G}{\partial \theta}^T + \sum K_i \frac{\partial P_i}{\partial \theta}^T\right), \quad (25)$$

it implies that P_G and P_i are to be optimized. Depending upon the sign of the coefficient K_G and K_i, the mobile robot is controlled in such a way to minimize or maximize the given performance index. In this example, K_G should be positive to minimize the distance between the robot and the goal, and K_i should be negative to maximize the distance between the robot and the obstacles. Here, the vector $\theta = \begin{bmatrix} x & y & \phi \end{bmatrix}^T$ denotes the posture variables of the mobile robot. When the angular velocity of the mobile robot is given, the homogeneous solutions make the mobile robot navigate.

Decision of K_G and K_i is made as follows. K_G depends on the distance and thus it is determined by experiment. K_i is determined by the following equation.

$$K_i = ke^{\frac{\ln(0.01)}{h}S_i}, \quad (26)$$

where k denotes weighting factor, h denotes permissible approach range, and S_i denotes the distance between the mobile robot and the *i-th* obstacle. K_i is equal to $0.01 \times k$ at $S_i = h$ according to (26). K_i should vary with respect to the distance from an obstacle to the robot, because obstacles outside of the permissible range are not needed to be cared, and the nearer obstacles should generate more input for the mobile robot. Fig. 11 shows that K_i varies with respect to the distance.

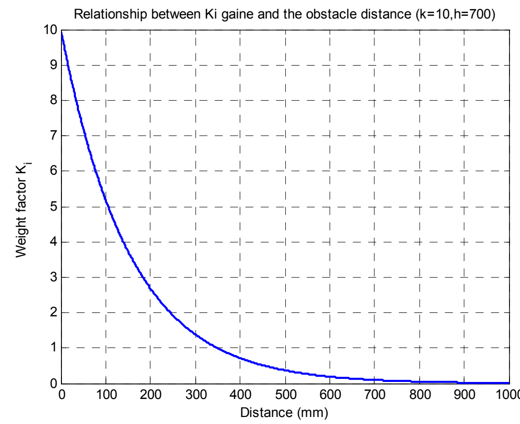

Fig. 11. Weight factor K_i property with respect to the distance.

B. Experiment

Experimentation has been performed to verify the navigation performance of the developed mobile robot. In the experiment, the odometry information was used for locating the mobile robot, and a laser range finder was used for detecting obstacles and map building.

Fig. 12 shows the experimental environment. The primary task is that the mobile robot starts at (0, 0) and moves to the goal point at (1000, 5000). While the mobile robot is navigating, it gathers the geometric information of the environment and the obstacles through a laser range finder. The results, the environment map and the trace of the mobile robot, are shown in Fig. 13. The curved line in the center of the map denotes the trace that the robot has been on, and the dots denote the environment.

In usual differential-driven mobile robots, the orientation of the mobile robot should be changed so that they avoid obstacles. This propagates additional error of the laser range finder due to the orientation change of the mobile robot. This problem can be removed by using omni-directional mobile robot, where the robot as well as the laser range finder is able to maintain its orientation, and thus the laser range finder is able to reduce the map building error. This point is one of merits of the omni-directional mobile robot in comparison to a usual differential-driven mobile robot.

The attached video clip demonstrates the navigation of the omni-directional mobile robot under fixed obstacles and moving obstacles.

Fig. 12. The picture of real environment

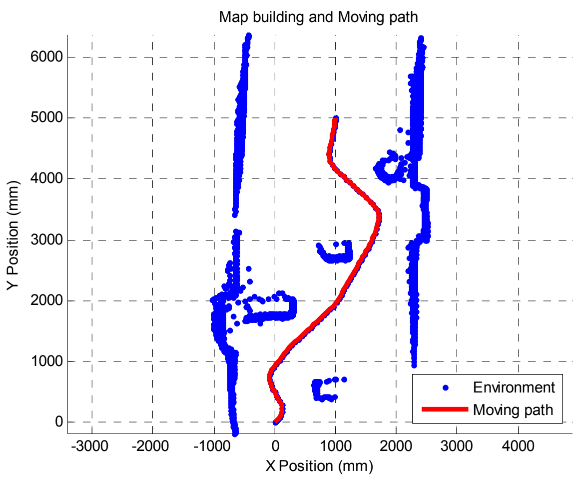

Fig. 13. The result of map building and navigation

V. CONCLUSION

In this paper, the navigation of an omni-directional mobile robot with three active caster wheels was investigated. We derived the odometry information from the parallel mobile geometry. The accuracy of the odometry information was measured by the external measurement system and the trajectory tracking performance was verified. Furthermore, we proposed a new navigation algorithm that simultaneously achieves the goal positioning and obstacle avoidance. The feasibility of this algorithm was verified through experimentation.

ACKNOWLEDGMENT

This work was supported by the GRRC Project of Gyeonggi Province Government, Republic of Korea (2007-041-0003- 001).

REFERENCES

[1] C. Campion, G. Batin, and B. D'Andrea-Novel, "Structural properties and classification of kinematics and dynamics models of wheeled Mobile Robot", *IEEE Trans. on Robot and Automation*, vol. 4, no. 2, pp. 281–340, 1987.

[2] P. F. Muir and C. P. Newman, "Kinematic modeling of wheeled mobile robot," *Journal of Robotics System*, vol. 4, no. 2, pp. 281–340, 1987.

[3] S. K. Saha and J. Angeles, "Kinematic and dynamics of a three-wheeled 2-DOF AVG," in *Proc. IEEE/RSJ Int. Conf. on Intelligent Robots and Systems*, pp. 1572-1577, 1989.

[4] P. Chen, S. Mitsutake, T. Isoda, and T. Shi, "Omni-directional robot and adaptive control method for off-road running," *IEEE Trans. on Robotics and Automation*, vol. 18, no. 2, pp. 251-256, 2002.

[5] K. Tadakuma, S. Hirose, and R. Tadakuma, "Development of VmaxCarrier2: omni-directional mobile robot with function of step-climbing," in *Proc. IEEE Int. Conf. on Robotics and Automation*, pp. 3111-3118, 2004.

[6] S. Ziaie-Rad, et al., "A practical approach to control and self-localization of Persia omni directional mobile robot," in *Proc. IEEE/RSJ Int. Conf. on Intelligent Robots and Systems*, pp. 3473-3479, 2005.

[7] J. E. M. Salih, et al., "Designing omni-directional mobile robot with mecanum wheel," *American Journal of Applied Sciences*, vol. 3, no.5, pp. 1831-1835, 2006.

[8] K. L. Moore and N. S. Flann, "A six-wheeled omnidiretional autonomous mobile robot," *IEEE Control System Magazine*, vol. 20, no. 6, pp. 53-66, 2000.

[9] M. D. Berkemeier and L. Ma, "Discrete control for visual servoing the ODIS robot to parking lot lines," in *Proc. IEEE Int. Conf. on Robotics and Automation*, pp. 3149-3154, 2005.

[10] M. Wada, A. Takagi, and S. Mori, "Caster drive mechanism for holonomic and omnidirectional mobile platforms with no over constraint," in *Proc. IEEE Int. Conf. on Robotics and Automation*, pp. 1531-1538, 2000.

[11] N. Ushimi, M. Yamamoto, and A. Mohri, "Two wheels caster type odometer for omni-directional vehicles," in *Proc. IEEE Int. Conf. on Robotics and Automation*, pp. 497-502, 2003.

[12] J. H. Lee, S. Yuta, E. Koyanagi, and B.-J. Yi, "Command system and motion control for caster-type omni-directional mobile robot," in *Proc. IEEE/RSJ Int. Conf. on Intelligent Robots and Systems*, pp. 2714-2720, 2005.

[13] B.-J. Yi and W.K. Kim, "The Kinematics for redundantly actuated omni-directional mobile robots," *Journal of Robotic Systems*, vol. 19, no. 6, pp. 255-267, 2002.

[14] R.A. Freeman and D. Tesar, "Dynamic modeling of serial and parallel mechanisms/robotic systems," Part I-Methodology, Part II-Applications, *20th ASME Biennial Mechanism Conf.*, Orlando, FL, pp. 7-27, 1988.

[15] K.H. Hunt, *Kinematic Geometry of Mechanisms*, Clarendon Press, Oxford, 1990.

[16] T.B. Park, J.H. Lee, B.-J. Yi, W.K. Kim, B.J. You, and S.R. Oh, "Optimal design and actuator sizing of redundantly actuated omni-directional mobile robots," in *Proc. IEEE Int. Conf. on Robotics and Automation*, pp. 732-737, 2002.

[17] P. Zavlangas, et al., "Fuzzy Obstacle Avoidance and Navigation for Omnidirectional Mobile Robots," ESIT 2000, pp. 375-382, September 2000, Aachen, Germany.